

# CurveALOHA: Non-linear Chirps Enabled High Throughput Random Channel Access for LoRa

Chenning Li, Zhichao Cao, Li Xiao

Michigan State University

{lichenni, caozc, lxiao}@msu.edu

**Abstract**—Long Range Wide Area Network (LoRaWAN), using the linear chirp for data modulation, is known for its low-power and long-distance communication to connect massive Internet-of-Things devices at a low cost. However, LoRaWAN throughput is far behind the demand for the dense and large-scale IoT deployments, due to the frequent collisions with the by-default random channel access (i.e., ALOHA). Recently, some works enable an effective LoRa carrier-sense for collision avoidance. However, the continuous back-off makes the network throughput easily saturated and degrades the energy efficiency at LoRa end nodes. In this paper, we propose CurveALOHA, a brand-new media access control scheme to enhance the throughput of random channel access by embracing non-linear chirps enabled quasi-orthogonal logical channels. First, we empirically show that non-linear chirps can achieve similar noise tolerance ability as the linear one does. Then, we observe that multiple non-linear chirps can create new logical channels which are quasi-orthogonal with the linear one and each other. Finally, given a set of non-linear chirps, we design two random chirp selection methods to guarantee an end node can access a channel with less collision probability. We implement CurveALOHA with the software-defined radios and conduct extensive experiments in both indoor and outdoor environments. The results show that CurveALOHA’s network throughput is 59.6% higher than the state-of-the-art carrier-sense MAC.

## I. INTRODUCTION

In the past decades, Bluetooth Low Power (BLE) [1], [2] and Zigbee [3], [4] radios have shown their success to build body area networks and wireless sensor networks (WSNs) for Internet-of-Things (IoT). Nowadays, billions of unattended IoT devices are scattered and connected in wide areas (e.g., industry, agriculture, city) [5]. A coming challenge is to scale the low-power IoT in these wide areas in a low-cost manner. To mitigate this gap, recent years have witnessed Low-power Wide-area Network (LPWAN) emerging as an attractive IoT architecture.

In multiple LPWAN techniques, LoRaWAN [6] is an open-source network standard operating on the unlicensed spectrum, in which LoRa end nodes communicate with LoRa gateways directly. From the bottom to the top, LoRa physical layer leverages Chirp Spread Spectrum (CSS) [7] to achieve long-distance and low-power data transmissions. For example, a commercial-off-the-shelf (COTS) LoRa gateway [8] can successfully demodulate data packet transmitted kilometers away whose signal-to-noise ratio (SNR) is as low as -20 dB [9]. A COTS LoRa radio [10] reaches the peak power consumption of 400 mW when transmitting at 20 dBm, but draws only 5  $\mu$ W in idle mode. Due to the long-distance and low-power

characteristics of LoRa links, LoRaWAN becomes a popular LPWAN protocol.

In LoRaWAN, given a physical channel and a configured Spreading Factor (SF) as the logical channel, an end node follows ALOHA media access control (MAC) to randomly access the media. ALOHA is simple to implement and has no extra energy consumption for maintaining any channel state. However, it exposes a risk of uncontrollable packet collision when network traffic becomes higher enough at a gateway, resulting in unexpected packet loss [11]. Although we can regulate the duty cycle of an end node by reducing it to 1% or less [12], ALOHA-enabled network throughput is far from the demand to support massive connections in the large-scale or densely deployed IoT [11], [13], [14].

Carrier-sense multiple access with collision avoidance (CSMA/CA) is a well-known scheme that outperforms ALOHA in terms of network throughput, and is widely adopted in wireless networks (e.g., WSNs [15], [16], Wi-Fi [17]). In CSMA/CA, carrier-sense is the key technology enabling an end node to detect the ongoing transmission in the channel, then it chooses a back-off to avoid the potential collision. For efficient CSMA in LoRa, LMAC [11] utilizes Channel Activity Detection (CAD) to balance the communication loads among the channels defined by frequencies and SFs. However, the continuous back-off significantly increases the packet delay which leads to a saturated network throughput that cannot meet system demand. Additionally, LMAC [11] reports that the energy overhead of continuous CADs is 20% to 25%, which significantly decreases the baseline of an end node’s lifetime.

In this paper, we propose CurveALOHA to achieve highly efficient random channel access in an SF channel without carrier sense. Beyond the linear chirp in the standard LoRa physical layer, CurveALOHA sits on a new physical layer that involves non-linear chirps. Given the special properties of a non-linear chirp, the transmissions over different non-linear chirps are quasi-orthogonal with each other and the linear one. Thus, they create new logical channels as the SF does for potential throughput gains, in which end nodes can select different non-linear logical channels to avoid packet collisions. After a logic channel is selected, end nodes schedule a transmission analogous to ALOHA. However, how to select the logical channels is non-trivial to fully exploit the advantages of the non-linear chirps.

To maximize the global network throughput by resolving

the logical channel selection, CurveALOHA proposes two versions with different network settings. The basic version (CurveALOHA-1) is to randomly select a logical channel each time. However, purely random selection cannot fully exploit the advantages of different types of non-linear chirps, which have different collision tolerance in real environments. To fully explore the packet collision pattern under certain traffic demand, we deliver the second version (CurveALOHA-2), in which each end node maintains the packet delivery ratio (PDR) for each logical channel and accordingly determines the probability of logical channel selection for packet transmission. In CurveALOHA-2, packet acknowledgment is a must to facilitate the PDR calculation locally.

We implement CurveALOHA with software-defined radios. Extensive experiments are conducted to verify the effectiveness of CurveALOHA. In comparison with the default ALOHA and state-of-the-art LoRa CSMA/CA-based LMAC [11], CurveALOHA achieves  $2.81 \times$  and  $1.6 \times$  network throughput, without any extra cost in energy consumption or computation efficiency. The main contributions are summarized as follows:

- We propose the idea of using non-linear chirps to create new logical channels, which can be utilized to improve the media access efficiency in LoRa.
- We propose CurveALOHA, a random selection scheme of the non-linear chirp logical channels, to significantly mitigate the packet collision of traditional ALOHA with zero extra overhead.
- We implement CurveALOHA on software defined radios and extensively evaluate its performance in real-life deployments. Results show that the network throughput can increase up to  $2.81 \times$  at a campus-scale scenario.

This paper is organized as follows. We introduce the related work in §II. In §III, the LoRa physical layer and our motivation are given, followed by the characteristics of non-linear chirps in §IV. The system designs of CurveALOHA can be found in §V. We present the system implementation and evaluation in §VI and VII, followed by the conclusion in §VIII.

## II. RELATED WORK

Recently, LoRaWAN [18] attracts massive research interests that focus on improving LoRaWAN performance for energy efficiency and coverage range. To achieve energy-efficient communication and large-range coverage, NELoRa [19] utilizes a deep neural network (DNN) to explore the multi-dimensional feature spaces of chirp signals while Charm [20] combines weak signals detected by a few gateways for coherently decoding. PLoRa [21] uses ambient LoRa excitations to achieve a long-distance passive LoRa backscatter. With the link traces of real LoRaWAN deployments in urban environments, DeepLoRa [22], LoSee [9], PolarTracker [23] and Silvia et al. [24] model the path loss of LoRa links which is further used for calibrating LoRa gateway deployment and adjusting LoRa link allocation. To enlarge LoRaWAN throughput or exploit non-linear chirps, some existing works are summarized as follows.

**Logical Channel Concurrency.** LoRaWAN uses the linear chirp modulation and multiplexes in one physical channel by setting different SFs (e.g., from 7 to 12). For an SF-specific linear chirp, NetScatter [25] subdivides it into multiple logical channels according to different start frequencies, delivering a larger network capacity by enabling concurrent transmissions of up to 256 devices on the different logical channels. However, NetScatter sacrifices the throughput of each logical channel. Besides, Tallal et al. [26], [27] use interleaved linear chirp modulation to increase the throughput by adding one more bit in a symbol. Unfortunately, the interleaved chirps significantly interfere with LoRa chirps when they have an identical SF. Thus the total number of logical channels is still limited in practice. In contrast, CurveALOHA relies on multiple types of non-linear chirps to increase the total number of logical channels while keeping the mutual interference as low as possible. Each non-linear chirp achieves equivalent throughput of the linear chirp and is more resilient to collisions.

**Collision Avoidance at MAC Layer.** Some works [11], [28], [29] have proposed LoRa frame scheduling protocols to avoid the potential collisions of LoRa transmissions. For example, DeepSense [28] enables LoRa carrier sense by training a DNN to detect whether LoRa signal exists and classify the corresponding configurations. To alleviate the computation cost on LoRa end nodes, LMAC [11] utilizes the low-cost CAD to replace DNN and allocates the physical channel and SF configuration based on the detected CAD and corresponding channel usage information. Piyare et al. [29] further propose a time division multiple access (TDMA) MAC protocol to increase the network throughput. However, either carrier sense of CSMA or time synchronization of TDMA needs extra control cost and unexpected delay, which is undesirable for low power LoRaWAN. CurveALOHA completely inherits ALOHA without any extra energy and computation overhead.

**Non-linear Chirp for Communication and Radar.** Several works [30]–[32] use the non-linear frequency modulation to improve the signal quality in radar systems. In addition, other works [33]–[35] utilize non-linear chirps to improve the channel access efficiency of wireless communication. However, CurveALOHA focuses on the design of non-linear chirps on the wide-area IoT for benefits of the network throughput, a brand-new scenario.

## III. LORAWAN PRELIMINARY

In this section, we illustrate the preliminary of the standard LoRa physical and MAC layers. First, LoRa physical layer specifies the symbol modulation and demodulation method with linear chirps. Second, with ALOHA MAC, collisions may frequently occur when two packets from two end nodes are overlapped.

### A. LoRa Physical Layer

In LoRa physical layer, a linear chirp is used to modulate bit-stream. As shown in Figure 1, LoRa has two kinds of linear chirps. One is up-chirp (e.g., red lines) whose slope is positive. The other is down-chirp (e.g., green line) with a negative slope.

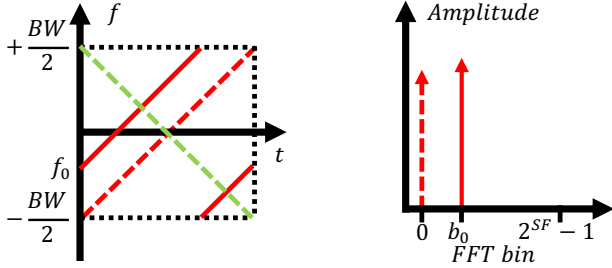


Fig. 1. The illustration of LoRa physical layer. The dashed red and green lines show base up- and down-chirps. The solid red line shows a modulated symbol using the shifted up-chirp. The right sub-figure shows the corresponding demodulation results after multiplying base down-chirp and applying FFT.

Two parameters, the bandwidth of narrowband  $BW$  and the time span  $T$ , decide the slope of the base up-chirp and down-chirp in the frequency-time domain, in which the frequency of the base up-chirp increases linearly from  $-\frac{BW}{2}$  to  $\frac{BW}{2}$ . And a base up-chirp  $h(t)$  can be indicated as follows:

$$h(t) = e^{j2\pi(-\frac{BW}{2}+kt)t} \quad (1)$$

where  $k$  is the slope of the base up-chirp  $\frac{BW}{T}$ . The base down-chirp is the conjugate of the base up-chirp  $h^*(t)$ . Moreover,  $T$  is determined by the configured  $SF$ . An up-chirp consists of  $2^{SF}$  chips (i.e., time slot unit) to represent  $SF$  bits. And each chip lasts  $\frac{1}{BW}$  second. Therefore, an  $SF$  up-chirp lasts for  $\frac{2^{SF}}{BW}$  seconds. Given a fixed  $BW$ , LoRaWAN allows adjusting  $T$  by setting  $SF$  from 7 to 12. When  $BW$  is  $125kHz$ , it takes about  $1ms$  and  $32.8ms$  to transmit an up-chirp by setting  $SF$  as 7 and 12.

At the transmitter side,  $SF$  bits can be modulated by a chirp symbol by adding the corresponding frequency shift  $f_0$  on the base up-chirp, which can be denoted as  $h(t)e^{j2\pi f_0 t}$ . As the solid red line shown in Figure 1, the start frequency of the modulated up-chirp is shifted up by  $f_0$ , and the frequencies higher than  $\frac{BW}{2}$  are moved down  $BW$ , which starts from  $-\frac{BW}{2}$ . For the demodulation at the receiver side, the basic idea is to multiply the shifted up-chirp symbol with the time synchronized base down-chirp. Given the start frequency  $f_0$ , the result is formulated as follows:

$$h^*(t)h(t)e^{j2\pi f_0 t} = e^{j2\pi f_0 t} \quad (2)$$

By applying the fast Fourier transform (FFT) on the result, a single peak appears at the FFT bin of  $b_0$  which corresponds to  $f_0$  in the frequency domain as the solid red arrow shown in Figure 1. Then  $SF$  bits can be decoded according to the unique matching between  $b_0$  and bit strings. Figure 1 also shows the peak of demodulated base up-chirp at the FFT bin of 0 (e.g., the dashed red arrow).

#### B. ALOHA MAC and Symbol Collision

In LoRaWAN, different LoRa end nodes adopt ALOHA to access the shared channel. In ALOHA, an end node can transmit its packet immediately without any back-off or carrier sense. Although ALOHA is simple to implement, it cannot maximize the network throughput due to packet loss in

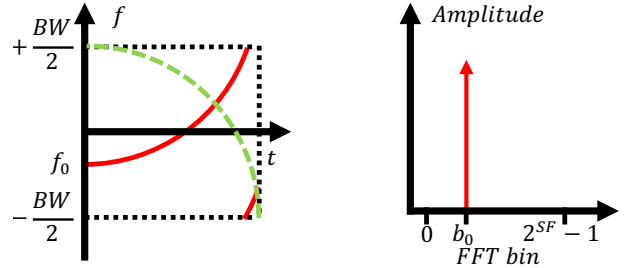


Fig. 2. The illustration of non-linear chirp-based modulation and demodulation. The solid red curve shows the frequency shift used to modulate data. We extract the energy peak to demodulate symbols by multiplying a base down-chirp (e.g., green dashed curve) and applying FFT.

collisions. For example, two LoRa packets from two different LoRa end nodes may frequently overlap with each other when they have similar duty cycle schedule. In theory, the maximum throughput of ALOHA is only 18.4% of the optimal channel capacity [36], [37]. As shown in Figure 1, we assume the encoded up-chirps of two different symbols are completely aligned and superposed. After multiplying the base down-chirp and applying FFT, two peaks appear at different FFT bins (e.g., 0 and  $b_0$ ). If the signal strength difference of the received symbols is large enough, only the symbol of the stronger signal can be correctly demodulated. Otherwise, no symbol can be reliably demodulated at all, leading to the packet loss which degrades the LoRaWAN throughput significantly. Since a LoRa consists of numerous symbols, the misalignment between two overlapped symbols will exhibit the same observation as the aligned ones.

## IV. NON-LINEAR CHIRP BASED LOGICAL CHANNEL

In LoRa, for each physical channel, different  $SFs$  are treated as logical channels [11], [38], which are orthogonal to each other and can be assigned to different end nodes to improve the network throughput. The larger the selected  $SF$  is, the larger a symbol on-air time is, resulting in larger energy consumption to transmit the data packet. Instead of using the  $SF$  as orthogonal logic channels in LoRa, CurveALOHA exhibits the opportunity to create new logic channels by exploring non-linear chirps under the same configured  $SF$ .

#### A. Non-linear Chirp based Modulation and Demodulation

We first demonstrate that non-linear chirps have the same modulation and demodulation mechanism at the symbol level. The base non-linear up-chirps are monotone curves which start at  $(0, -\frac{BW}{2})$  and end at  $(\frac{2^{SF}}{BW}, \frac{BW}{2})$ . We use  $f(x)$  to indicate the shape of a non-linear chirp. Given the base non-linear up-chirp, as shown in Figure 2, we modulate data by shifting its initial frequency to  $f_0$  as the linear up-chirp does. For demodulation of non-linear chirps, we first align the symbol to a base down-chirp (e.g., green dashed curve) and then multiply it to extract the initial frequency  $f_0$  by using FFT. For simplicity, we call this process as *dechirp*. In this way, given the same configured  $BW$  and  $SF$ , non-linear chirps deliver the same throughput as the linear ones in case of no collisions.

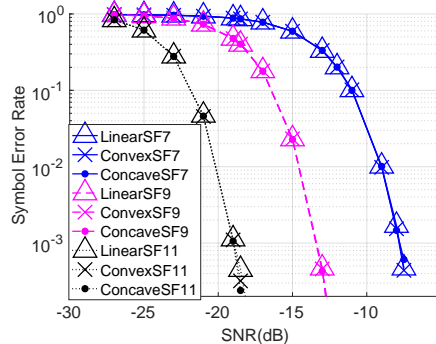


Fig. 3. The SER distribution of different types of chirps under various SNR conditions.

### B. Comparable Noise Tolerance

The dechirp of LoRa aims to accumulate the spectral energy of linear chirps into a single frequency, thus it can suppress the interfered random noise and guarantee the demodulation even at extremely low SNR conditions. We demonstrate that non-linear chirps retain the inherent noise resilience of linear ones in the dechirp. To analyze the noise tolerance of the non-linear chirps, we empirically study the symbol error rate (SER) in LoRa transmission under various SNR conditions, in which various white Gaussian noise (AWGN) is added to the encoded up-chirps [39], [40]. Specifically, we use Monte Carlo simulation and compare both convex up-chirp (i.e.,  $f(x) = x^2$ ) and concave up-chirp (i.e.,  $f(x) = 2x - x^2$ ) with the LoRa linear chirp under three different SF configurations (i.e., 7, 9, 11). We manually align the up-chirp symbols to the corresponding base down-chirp for demodulation. For each scenario, we run 100,000 times to calculate the average SER. Illustrated in Figure 3, the SER-SNR trend under different types (e.g., linear, convex, concave) of up-chirps is quite similar under the same SF. For example, the SNR of the received signal should be larger than about -7.5 dB to ensure SER is lower than 0.1% for all three types of chirps when SF is 7. Similarly, when SF becomes 9 and 11, the SNR thresholds are about -12.5 dB and -17.5 dB, respectively. Overall, the non-linear chirps keep the strong noise tolerance as the linear chirp does.

### C. Accounting for Collisions with Logical Channels

Whether different types of linear and non-linear chirps can coexist with each other in collisions is the key point to be assigned as the logical channel for concurrent transmissions.

To illustrate the advantages of non-linear chirps, we first give the following example with the overlapped *reference signal*  $C_r$  and the *interference signal*  $C_i$  in Figure 4. To demodulate  $C_r$ , we then adopt the dechirp on the collided chirp signals. Figure 4 shows the spectral energy distribution of two chirps. And  $p_r$  indicates the amplitude of the FFT bin corresponding to the shifted initial frequency for  $C_r$ . When an up-chirp and a base down-chirp have different types of curves, the frequency domain energy is no longer accumulated at a single bin but scattered over multiple bins. We use  $p_i$  to

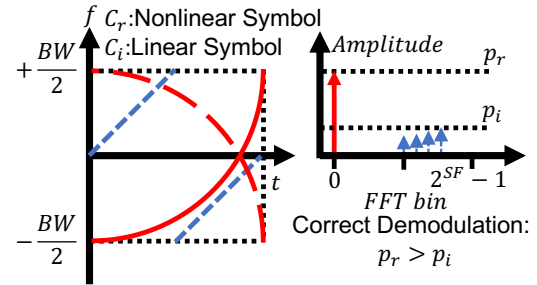


Fig. 4. Concurrent demodulation opportunity between two collided symbols using two types of chirps as the logical channels.

indicate the highest amplitude among a series of FFT bins that are derived by multiplying the  $C_i$  symbol with the conjugate of  $C_r$ . To guarantee the  $C_r$  symbol to be correctly demodulated,  $p_r$  should be higher than  $p_i$ . Then the signal-interference ratio (SIR) is defined to indicate the interference of  $C_i$  over  $C_r$  as SNR does. And we can define the largest power difference of chirp symbols  $C_r$  and  $C_i$  as a SIR threshold  $SIR_{C_r}(C_i)$  by setting  $p_r = p_i$ , above which the reference signals can be decoded.

**Remark.** The rationale of CurveALOHA is that by scattering the spectral energy of those interfered chirps with different types in the dechirp, taking different types of non-linear chirps as logical channels can support a lower SIR threshold for weak signal demodulation in collisions, enabling a larger network throughput than the baseline of LoRaWAN.

**Validation.** To estimate the SIR threshold  $SIR_{C_r}(C_i)$  given different types of non-linear chirps as logical channels, we utilize the Monte Carlo method to uniformly traverse the overlapping scenarios with random time offsets and gradually decrease SIR between  $C_r$  and  $C_i$  from -1 dB to -30 dB. Given a SIR and the chirp types (e.g., SF, BW, and shapes) of  $C_r$  and  $C_i$ , we randomly generate the encoded chirp symbols of  $C_r$  and  $C_i$ . The reference base down-chirp symbol is aligned to the reference up-chirp manually for demodulation. And a symbol error occurs when we fail to demodulate the  $C_r$  symbol under these settings. We do not stop running the simulation until we observe 100 symbol errors under each setting. Then, SER is calculated as the ratio between 100 and the total rounds we have run. After getting a SIR below which the SER of the reference signal is higher than 1%, we recognize the SIR as the SIR threshold.

We further select five polynomial functions to form the logical channel pool for concurrent transmissions, including *linear*: $f(x) = x$ , *quadratic1*: $f(x) = x^2$ , *quadratic2*: $f(x) = 1 - (x - 1)^2$ , *quartic1*: $f(x) = x^4$  and *quartic2*: $f(x) = 1 - (x - 1)^4$ . Thus we have 5 logical channels to calculate the SIR threshold with each other for each configured SF. The resulting SIR threshold heatmap is shown in Figure 5. And we can observe that:

- 1) **For all SFs, when  $C_r$  and  $C_i$  are the same, the SIR thresholds of non-linear logical channels are much lower than that of the linear one.** The SIR threshold between two linear chirps is approximately 0 dB, which means only the

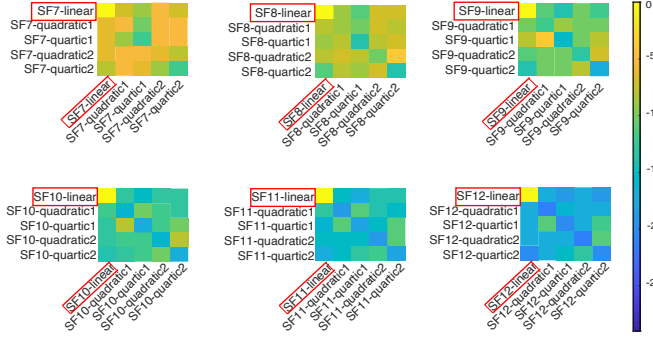


Fig. 5. SIR threshold heatmap of 5 chirps with the same SF. Each block indicates the SIR threshold of a reference signal (i.e., row mark) under an interference signal (i.e., column mark). The rectangle denotes the LoRa linear chirps. With a darker color, the block corresponds to a lower SIR threshold.

stronger signal can be successfully demodulated. In contrast, the non-linear logical channel can resist self-interference with a lower SIR threshold. For quadratic chirps, when SF is 12, the SIR threshold under self-interference is as low as -16 dB. This indicates that non-linear logical channels are more resilient to self-interference than linear ones.

**2) For all SFs when  $C_r$  and  $C_i$  are different, the SIR thresholds exhibit a loose requirement to concurrently demodulate the weak signal.** The SIR threshold between two different logical channels is lower than -5 dB, which indicates a weak signal can be successfully demodulated if its SIR is larger than -5 dB. As SF increases, the SIR threshold between two different logical channels becomes lower (i.e., the color becomes darker). The results show certain orthogonality among these logical channels. As a result, the transmissions on one logical channel are less interfered with by others on a different logical channel.

**Remark.** Given the non-linear chirp-based modulation and demodulation design, non-linear chirps can be used for long-range low-power communication as the linear chirp does. Besides, they create new logical channels which are quasi-orthogonal with each other and the linear one. Thus concurrent transmissions using different logical channels are less interfered with each other, enabling simultaneous demodulation.

## V. SYSTEM DESIGN

Sitting upon our non-linear chirps at the physical layer, we have multiple logical channels under the same SF for MAC layer design. Our problem can be formulated as given  $n$  available logical channels (i.e.,  $\{C_1, C_2, \dots, C_n\}$ ) when an end node has a packet to transmit at time  $t$ , it selects one logical channel  $C(t)$  to transmit the packet immediately without carrier sense or transmission scheduling. According to our observation in §IV-C, the logical channels are quasi-orthogonal, which means several collided packets can be concurrently demodulated when the SIR thresholds among the used logical channels can be met. In LoRaWAN, end nodes usually do not know the traffic schedule of others and whether the SIR thresholds can be met at the gateway. Therefore, a collision-free guarantee is hard to achieve without any network

status. However, it needs extra costs to maintain the knowledge of network status. CurveALOHA consists of two versions to minimize the packet collision possibility in different levels with different prior knowledge to be maintained.

### A. CurveALOHA-1

CurveALOHA-1 is a simple version. An end node does not need to have any knowledge of network status. The selection strategy is the *random selection*. The end node just randomly selects  $C(t)$  from  $\{C_1, C_2, \dots, C_n\}$ . The probability  $p_k$  of selecting a logical channel  $C_k$  ( $k \in [1, n]$ ) is uniform as  $1/n$ . The selection event is independent each time.

**Performance Analysis:** We suppose the transmissions of two end nodes  $\alpha$  and  $\beta$  collide at time  $t$ .  $\alpha$  and  $\beta$  select logical channel  $C_\alpha(t)$  and  $C_\beta(t)$ , respectively. If the mutual SIRs between  $\alpha$ 's and  $\beta$ 's packets are larger than the below 0 dB SIR thresholds  $SIR_{C_\alpha(t)}(C_\beta(t))$  and  $SIR_{C_\beta(t)}(C_\alpha(t))$ , the two packets can be concurrently demodulated. However, in traditional LoRWAN with only the linear chirp logical channel, only the stronger signal has the chance to be demodulated. Therefore, CurveALOHA-1 can achieve higher network throughput than ALOHA. On the other hand, without any network status, the selection of  $C_\alpha(t)$  and  $C_\beta$  may fail to meet the SIR requirements. Therefore, without properly utilizing the quasi-orthogonality among the logical channels, the network throughput is not optimal.

### B. CurveALOHA-2

Based on the uniform selection strategy in CurveALOHA-1, CurveALOHA-2 assigns a weight  $w_k$  for each logical channel  $C_k$  ( $k \in [1, n]$ ) to adjust its selection probability accordingly. The probability  $p_k$  is calculated as follows:

$$p_k = \frac{w_k}{\sum_{j=1}^n w_j} \quad (3)$$

The weight  $w_k$  is initialized as  $1/n$ , then it is continuously updated with the SIR thresholds under the interference of other logical channels and the packet delivery ratio (PDR) observed from transmissions over the logical channel  $C_k$  in a period. Given an SF configuration,  $SIR_k^{\max}$  and  $SIR_k^{\min}$  indicate the maximum and minimum SIR thresholds between the reference signal of  $C_k$  and the interference signals of others, as shown in the  $C_k$  row of the heatmap in Figure 5. These two values indicate  $C_k$ 's ability to improve concurrent transmission under the inference of others. They are constant, thus can be pre-calculated and hard-coded into the communication stack without any online calculation and update.

$P_k$  indicates the PDR for transmissions over  $C_k$  in the local view. For example, if an end node transmits 5 packets over  $C_k$  and 4 of them are successfully demodulated by gateways,  $P_k$  is 0.8. Given the PDR  $P_k$ , the corresponding selection probability  $p_k$  is updated using exponentially weighted moving average (EWMA) method [41]. Specifically,  $P_k(m)$  is the PDR newly measured in period  $m$  for the logical channel  $C_k$  (e.g., 5 new packets are transmitted). In next period  $m + 1$ , the

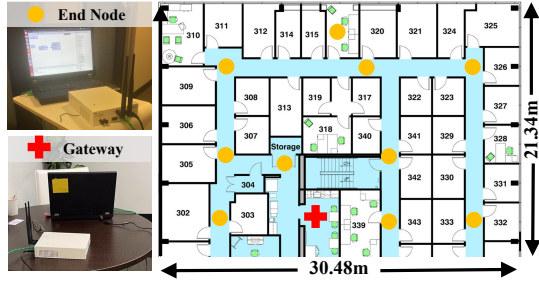


Fig. 6. The indoor office with the scattered end nodes.

probability  $p_k(m+1)$  for the logical channel  $C_k$  to be selected is calculated as:

$$p_k(m+1) = \kappa p_k(m) + (1 - \kappa) P_k(m) \quad (4)$$

where  $\kappa$  is a constant factor between 0 and 1 to determine how important the historical observation is. A large  $\kappa$  emphasizes the historical value. We set  $\kappa$  as 0.2 to emphasize the newly observed estimation as LMAC [11] does. When the  $p_k(m+1)$  is updated, the  $w_k(m+1)$  is calculated as:

$$w_k(m) = w_k(m) \times \tau^{1-P_k(m)/P_{thres}} \quad (5)$$

$$w_j(m+1) = w_j(m) \times \delta_j(C_k), \text{ for } j = 1, \dots, n \quad (6)$$

where  $\delta(C_k)$  corresponds to absolute value of the SIR threshold obtained in Figure 5. For example, when  $P_k(m)$  is smaller than a PDR threshold  $P_{thres}$ , we find the column of the SIR threshold map in which the current logical channel  $C_k$  has the highest SIR threshold (e.g., -5dB) as the reference channel. As a result, each kind of logical channel can adapt its weight based on the SIR threshold in the column. Otherwise, we select the column in which the current logical channel  $C_k$  has the lowest SIR threshold (e.g., -15dB) as the reference channel to increase its probability to be selected. As a result, CurveALOHA reuses the Equation (3) to calculate the probability of those logical channels for the next round.  $\tau$  is a constant decay factor between 0 and 1 to adjust the weight  $w_k$  according to the newly measured and updated PDR. The PDR threshold  $P_{thres}$  is 0.8 by default.

**Performance Analysis:** We show how  $P_k(m)$  and the SIR thresholds adjust the weight  $w_i$ . in Equation 5,  $p_k(m+1)$  increases with a  $P_k(m)$  larger than  $P_{thres}$ . Since  $\tau$  is between 0 and 1,  $\tau^{1-P_k(m)/P_{thres}}$  is larger than 1 when  $P_k(m)$  reach the PDR threshold. Hence, the new estimated weight gets larger as well. Additionally, when  $P_k(m)$  is higher than  $P_{thres}$ , the logical channel  $C_k$  should be rewarded. Since SIR thresholds are smaller than zero, a lower SIR threshold indicates better PDR even the interference from other logical channel is strong. When the link quality is good, we use the absolute value of  $SIR_k^{\min}$  to further enhance the weight  $w_k$ . As a result, we have higher chance to select this temporal good channel than others. Otherwise, we use  $|SIR_k^{\min}|$  to reduce the  $w_k$ . We also reward different logical channels according to their SIR thresholds. The better a logical channel is currently, the higher its weight is. Finally, we can obtain an optimal selection weight to adapt the local traffic pattern and the corresponding SIR constraints

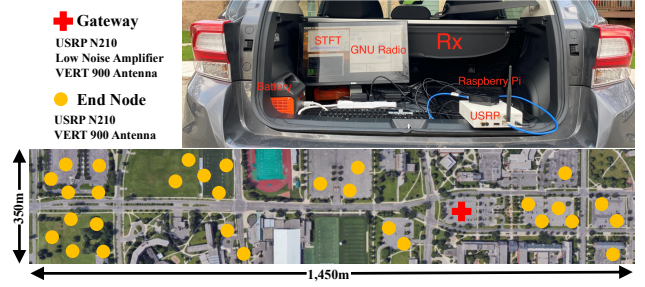


Fig. 7. Bird view of the outdoor campus and deployment.

with other end nodes. Therefore, the network throughput of CurveALOHA-2 must be higher than CurveALOHA-1. To measure the  $P_k(m)$ , we need the acknowledgment from the gateway, which incurs extra cost at the gateway side compared with CurveALOHA-1.

## VI. IMPLEMENTATION

We implement CurveALOHA on the software-defined radio (SDR) platform, namely USRP N210 with a UBX daughterboard, operating at the 904.0MHz ISM band. The UHD+GNURadio [42] is adopted to launch the modulation/demodulation and monitor the carrier spectrum using real-time Short Time Fourier Transform (STFT). All radios are equipped with a VERT900 antenna [43] to enhance below-GHz ISM band signal transmissions and receptions. By default, our experiment uses the spreading factor SF = 10 and bandwidth BW = 125 kHz, at the sampling rate of 1 MHz.

For each packet, a 25-bytes payload is transmitted and evaluated at the gateway. And modulation and demodulation algorithms are achieved in MATLAB and hardware-independent to be implemented on any commercial LoRa gateways as long as the physical samples can be obtained. In comparison with the COTS LoRa gateway, our demodulation method does not have a receiving-buffer overflow problem. Additionally, the message-in-message (MIM) [44], referring to the preamble of a latter coming packet is still can be captured, is enabled during packet demodulation. With MIM, the strong signals among the collided signals may be decoded.

**Baseline methods.** We apply CurveALOHA to LoRaWAN which is the prevalent data MAC layer protocol primarily based on ALOHA. The original LoRaWAN ALOHA only using the linear chirp is also adopted as the baseline. Four types of non-linear chirps are evaluated as the non-linear chirp pool: *quadratic1*:  $f(x) = x^2$ , *quadratic2*:  $f(x) = -x^2 + 2x$ , *quartic1*:  $f(x) = x^4$ , *quartic2*:  $f(x) = -x^4 + 4x^3 - 6x^2 + 4x$ . We do not involve linear chirp due to its high SIR threshold (0 dB) under the interference of itself. As LoRaWANs are constrained by the channel access time requirements ( $\leq 1\%$  duty cycle ratio for each end node, etc.), it is difficult to experimentally show the full advantage of CurveALOHA with a limited number of end nodes. Instead, we conduct trace-driven emulation to exhibit the LMAC advantage for a scaled LoRaWAN network [11].

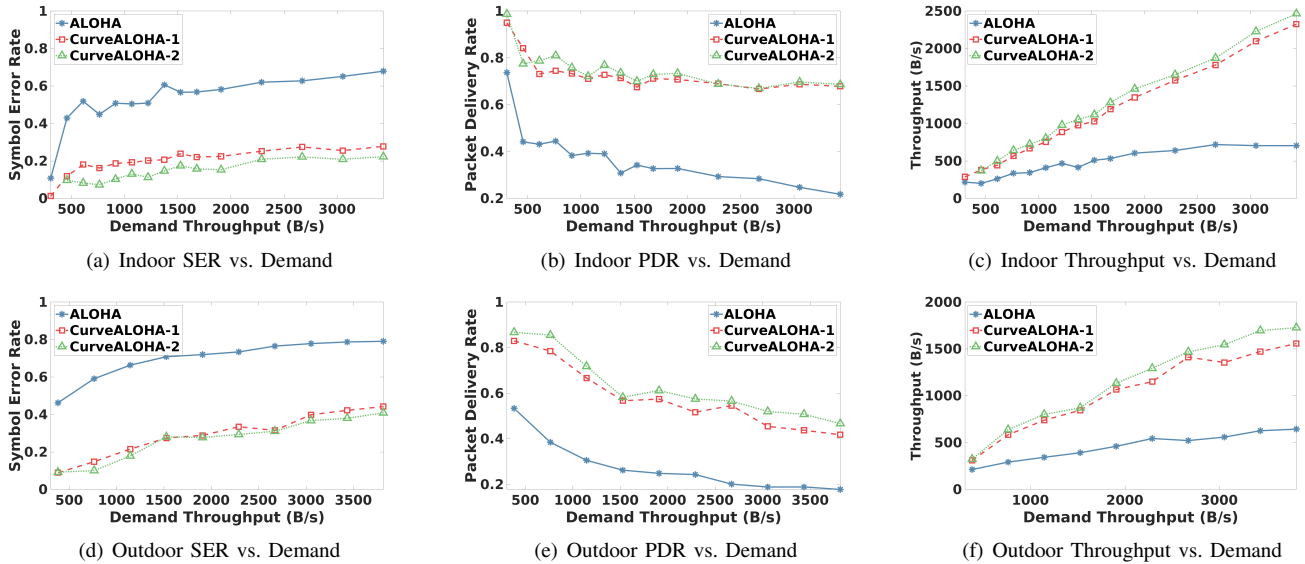


Fig. 8. Network performance comparison among ALOHA and CurveALOHA on SER, PDR, and throughput for indoor (top) and outdoor (bottom) experiments.

**Deployment environments.** First, we deploy the transmitter and gateway in an office building. As shown in Figure 6, the office building is  $30.48m \times 21.43m$  large and consists of multiple rooms and some concrete walls in or between them. We place the gateway in the kitchen and move the transmitter to 10 different locations for data collection. At each location, we configure the transmitter to send LoRa packets in different spreading factors and chirp symbol settings. In addition, we deploy CurveALOHA in our campus. Illustrated in Figure 7, we deploy the gateway powered by a portable battery on a parking lot and move the transmitter to 30 locations. By default, we use the outdoor dataset for evaluations.

**Evaluation Metrics.** Three metrics are adopted to evaluate CurveALOHA. The first is **SER** which indicates the symbol-level demodulation accuracy [39], [40]. The second is **Packet Delivery Rate (PDR)** which calculates the end-to-end packet reception rate. With the redundant coding and forward error correction (FEC), a packet can be treated as received when at least 80% of symbols can be decoded successfully.<sup>1</sup> The third one is **Network Throughput** indicating the amount of payload data successfully delivered per second, denoted by B/s (Byte/second). Since the power supply and decoding latency are usually not big concerns at the gateway side of the LPWAN networking stack, we do not consider the performance of energy consumption and the computation efficiency [19].

## VII. EVALUATION

In this section, we first evaluate CurveALOHA in indoor and outdoor experiments. Then the per-node performance is analyzed to evaluate its fairness and robustness, under different SNR conditions. Finally, based on the collected data, we conduct the parameter analysis to verify the effectiveness of CurveALOHA in various scenarios.

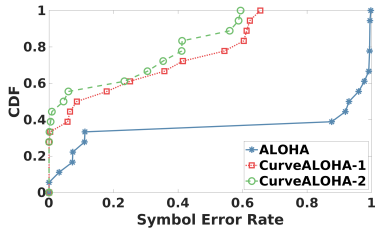
<sup>1</sup>Most error correction codes can successfully recover a LoRa packet when the SER is as high as 20% [45].

### A. Overall Performance and Comparison

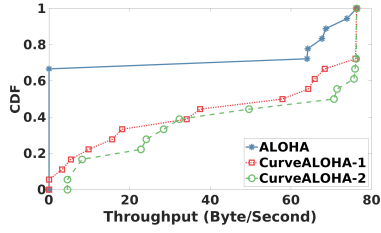
**Indoor Experiments.** We first compare CurveALOHA with the standard ALOHA when network demand varies in the indoor experiment, shown in Figure 8(a) to 8(c). In accordance with our design (§V), we observe that both two versions of CurveALOHA outperform the baseline ALOHA significantly. In comparison with ALOHA, Figure 8(a) shows that CurveALOHA-1/2 decreases the SER to 27.85% and 22.28% from 67.91% of ALOHA when the demanded throughput is around 3,400 B/s, which demonstrates the effectiveness of involving non-linear chirps to deliver data more efficiently. Thus CurveALOHA can support larger concurrency by delivering a higher throughput in Figure 8(c). For example, the corresponding improvement of throughput is 3.31 $\times$  and 3.43 $\times$ . In Figure 8(b), ALOHA PDR is below 60% with a network demand larger than 400 B/s. And it decreases slowly to 0.2 until the network demand is increasing to 3,000 B/s. In contrast, the PDRs of CurveALOHA are maintained above 65%, even with the network demand up to 3,400 B/s.

Overall, CurveALOHA outperforms ALOHA through the multiple non-linear chirps created logical channels and achieves up to 60% SER reduction and 3.37 $\times$  throughput improvement at the demanded throughput of 3,400 B/s, while maintaining the PDR above 65%.

**Outdoor Experiments.** We further conducted a set of experiments in our university area to investigate the feasibility of CurveALOHA, in which the collected signals have more dynamics in background noise difference and power attenuation difference. Illustrated in Figure 8(d) to 8(f), both versions of CurveALOHA keep the SER under 20% when the demand throughput increase to 1,200 B/s while it is around 70% for ALOHA. Such an optimized SER in Figure 8(d) delivers high PDR and throughput. Figure 8(e) shows that CurveALOHA-1/2 achieves up to 2.35 $\times$  and 2.66 $\times$  increment of PDR with the demanded throughput of 3,700 B/s. And the correspond-



(a) CDF of SER across nodes



(b) CDF of Throughput across nodes

Fig. 9. CDFs of the per-node network performance (demand 1,400 B/s).

TABLE I  
COMPARISON OF THROUGHPUT GAINS AGAINST ALOHA

Demand (B/s)	1,000	1,500	2,000	2,500	3,000	3,500
LMAC-2 <sup>a</sup>	2.22×	1.83×	1.70×	1.76×	1.81×	1.87×
CurveALOHA-2	2.33×	2.22×	2.38×	2.81×	2.76×	2.70×

<sup>a</sup>Results reported in Figure 13a of LMAC [11].

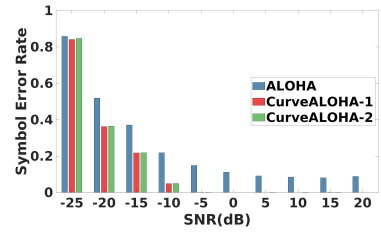
ing throughput gain is  $2.41\times$  and  $2.71\times$ , respectively.

Overall, as the demanded throughput goes up, the gains of PDR and throughput for CurveALOHA increase gradually, spanning from  $2.25\times$  to  $2.71\times$  for the demanded throughput of 1,000 to 3,700 B/s. This outperforms LMAC [11] in the comparable demands, which improves the throughput by  $1.52\times$ ,  $1.87\times$ , and  $2.21\times$  for three versions at the demand of 3,500 B/s, respectively. The statistical comparison can be referred to as § VII-B. However, CurveALOHA only relies on the design and selection of non-linear chirps, instead of using different channel/SF with a time-consuming collision avoidance scheme.

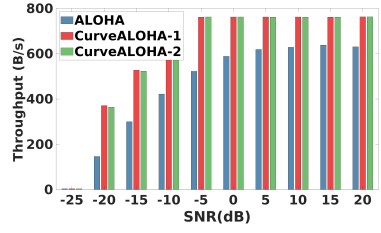
**Remarks.** The above experiments demonstrate the advantage of CurveALOHA on improving the network throughput in real environments. Although the standard ALOHA cannot deal with the collided transmissions with significant power differences in SIRs, CurveALOHA achieves superior collision resolving by fully utilizing non-linear chirps.

### B. Comparison Study

LMAC [11] is the state-of-the-art CSMA/CA-based LoRa MAC layer protocol. Although LMAC-3 has higher throughput than LMAC-2, it needs the gateway to share the global view channel utilization periodically. To fairly compare CurveALOHA with LMAC, we use CurveALOHA-2 and LMAC-2. They both use local observed network status to optimize channel selection. In Table I, we separately list the network throughput gains of CurveALOHA-2 and LMAC-2 in different demand throughput. The results of LMAC-2 are



(a) SER vs. SNR



(b) Throughput vs. SNR

Fig. 10. Noise resilience under various SNR conditions (demand 763 B/s).

reported in its paper. We can see CurveALOHA-2 outperforms LMAC-2 in all demand throughput settings. CurveALOHA-2 can achieve 59.6% higher throughput than LMAC-2 when the demanded throughput is 2,500 B/s. The reason is that the continuous backoff of LMAC-2 incurs extra time delay which could reduce the network throughput, but CurveALOHA-2 allows end nodes to immediately access the channel without any backoff.

### C. Fairness and Robustness of CurveALOHA

To verify the fairness of CurveALOHA's performance, a closer look at the per-node results is provided for more insights into the advantages of CurveALOHA over ALOHA. Figures 9(a) and 9(b) show the cumulative distribution functions (CDFs) of the per-node network performance metrics. We can see that majority of ALOHA nodes suffer high SER, half of which have more than 95% of SER. Thus the resulting throughput is lower than 10 B/s for half nodes. And the remaining ALOHA nodes achieve throughput scattered from 20 B/s to 80 B/s. In contrast, the CDFs of CurveALOHA do not exhibit undesirable long tails with a steeper trend. For example, 60% of CurveALOHA's nodes deliver an SER under 20% and network throughput is mostly larger than 60 B/s. The above results suggest that CurveALOHA achieve better balance and fairness against the standard ALOHA in utilizing the shared communication medium.

To further understand the robustness of CurveALOHA on collision resolving, we evaluate the noise resilience of CurveALOHA under diverse SNR conditions. Note that for fine-grained SNR control, we add white Gaussian noise with controlled amplitudes to the collected I and Q traces of packets [39], [40]. Figure 10(a) and 10(b) shows that CurveALOHA achieve consistent improvement as the SNR decreases from 20dB to -20dB. The rationale is that non-linear chirps cannot only suppress the background noise by focusing the spectral energy of the target chirp signals as linear chirp but

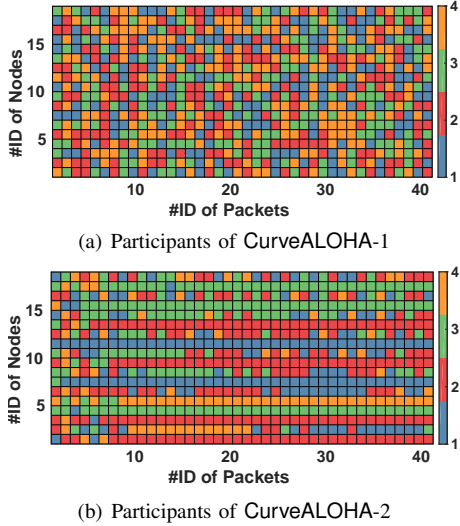


Fig. 11. Participant selection of non-linear chirps in various nodes and packets for CurveALOHA-1/2.

TABLE II  
THROUGHPUT GAINS FOR SPREADING FACTOR (DEMAND 3,000 B/s)

Setting	SF7	SF8	SF9	SF10	SF11	SF12
CurveALOHA-1	2.00×	2.06×	2.24×	2.73×	3.31×	3.52×
CurveALOHA-2	2.07×	2.12×	2.31×	2.83×	3.52×	3.78×

also reduce the interference of collided signals by scattering their energy on the spectrum (§ IV-C).

#### D. Parameter Study

**Spreading Factor.** We first evaluate CurveALOHA’s performance under various SF configurations, using data collected from the indoor experiment. Illustrated in Table II, CurveALOHA achieves consistent improvement on network throughput against ALOHA. And the throughput gain increases with a larger SF, up to 3.52× and 3.78× for SF=12, respectively. The significant throughput improvement is attributed to the lower SER of non-linear chirps, reducing 70% of ALOHA to 17.60% and 14.65%. This is consistent with our analysis in Figure 5, in which non-linear chirps can achieve a lower SIR threshold for a larger SF. Thus CurveALOHA can support more concurrency of transmissions, especially those collided signals with significant power differences.

**Decay Factor.** CurveALOHA-2 performs better than CurveALOHA-1 for most scenarios due to its active participant selection of non-linear chirps. We evaluate the processing and impact of the convergence of CurveALOHA-2. Figure 11 first illustrates the selection processing from the pool of four non-linear chirps (MATLAB pcolor function) when 18 nodes transmit 40 packets alternatively. In comparison with the random selection of CurveALOHA-1, CurveALOHA-2 adaptively adjusts the selection possibility of each node locally, based on the PDR estimated by the SER calculated from each packet. Thus it can always select the optimal type of non-linear chirp by fully utilizing the local information (§ V).

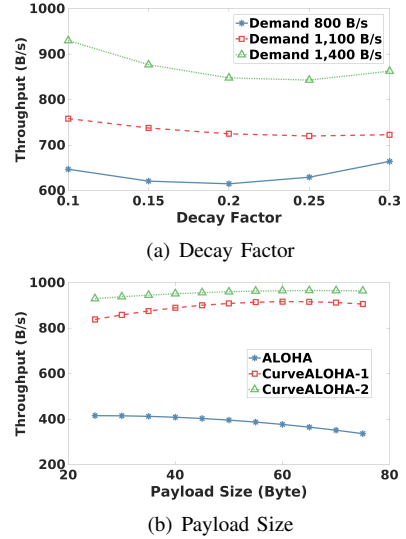


Fig. 12. Achieved throughput vs. various decay factors for CurveALOHA-2 and payload size with demand throughput of 1,400 B/s.

We further evaluate the impact of the decay factor in Equation (5), which controls the local convergence speed of CurveALOHA-2 nodes. Figure 12(a) shows a smaller decay factor achieves a larger throughput since CurveALOHA-2 converges faster, especially for a larger demand throughput of 1,400 B/s. A larger decay factor can also improve the performance by guaranteeing an unstable selection and avoiding the local optimal selection.

**Payload Size.** Varying payload size can evaluate the impact of long packets, under kinds of timing offsets. Figure 12(b) shows that ALOHA suffers from a longer packet with larger payloads. And even a small signal offset can induce the decoding error in resolving collisions. However, CurveALOHA-1/2 performs consistently or even better due to the lower SIR threshold of non-linear chirps for collision resolving (§ IV-C).

## VIII. CONCLUSION

In this paper, we present CurveALOHA to boost the LoRaWAN throughput by creating more logical channels with non-linear chirps. First, we design the modulation and demodulation schemes of non-linear chirps and validate that non-linear chirps can achieve comparable performance in terms of noise tolerance. Then, we demonstrate the feasibility of using these non-linear chirps to create new logical channels. The low SIR thresholds among collided non-linear chirps enable quasi-orthogonal logical channels. Finally, we propose two versions of MAC protocols to maximize the network throughput at different levels for non-linear logical channel selection. We implement CurveALOHA with SDRs and evaluate its performance in both indoor and outdoor environments. Experimental results show that CurveALOHA can achieve 1.6× LoRaWAN throughput of state-of-the-art LMAC [11].

## ACKNOWLEDGEMENT

This study is supported in part by NSF Awards CNS-1909177.

## REFERENCES

- [1] A. K. Das, P. H. Pathak, C.-N. Chuah, and P. Mohapatra, "Uncovering privacy leakage in ble network traffic of wearable fitness trackers," in *Proceedings of ACM MobiSys*, 2016.
- [2] K. E. Jeon, J. She, P. Soonsawad, and P. C. Ng, "Ble beacons for internet of things applications: Survey, challenges, and opportunities," *IEEE Internet of Things Journal*, vol. 5, no. 2, pp. 811–828, 2018.
- [3] L. Mo, Y. He, Y. Liu, J. Zhao, S.-J. Tang, X.-Y. Li, and G. Dai, "Canopy closure estimates with greenorbs: sustainable sensing in the forest," in *Proceedings of ACM SenSys*, 2009.
- [4] X. Mao, X. Miao, Y. He, X.-Y. Li, and Y. Liu, "Citysee: Urban CO<sub>2</sub> monitoring with sensors," in *Proceedings of IEEE INFOCOM*, 2012.
- [5] D. Magrin, M. Centenaro, and L. Vangelista, "Performance evaluation of lora networks in a smart city scenario," in *Proceeding of IEEE ICC*, 2017.
- [6] L. Alliance, "Lorawan specification," <https://lora-alliance.org/about-lorawan>, accessed 08-Apr-2020.
- [7] R. Eletreby, D. Zhang, S. Kumar, and O. Yağan, "Empowering low-power wide area networks in urban settings," in *Proceedings of ACM SIGCOMM*, 2017.
- [8] Semtech, "Lora sx1255," <https://www.semtech.com/products/wireless-rf/lora-gateways/sx1255>, accessed 07-Apr-2020.
- [9] Y. Yao, Z. Ma, and Z. Cao, "Losee: Long-range shared bike communication system based on lorawan protocol," in *Proceedings of EWSN*. Junction Publishing, 2019.
- [10] Semtech, "Sx1276/77/78/79 datasheet," <https://www.semtech.com/products/wireless-rf/lora-transceivers>, accessed 08-Apr-2020.
- [11] A. Gamage, J. C. Liando, C. Gu, R. Tan, and M. Li, "Lmac: efficient carrier-sense multiple access for lora," in *Proceedings of ACM MobiCom*, 2020.
- [12] E. S. R. Devices, "Operating in the frequency range 25 mhz to 1000 mhz; part 1: Technical characteristics and methods of measurement," *European Telecommunications Standards Institute*, 2017.
- [13] B. Ghena, J. Adkins, L. Shangguan, K. Jamieson, P. Levis, and P. Dutta, "Challenge: Unlicensed lpwans are not yet the path to ubiquitous connectivity," in *Proceedings of ACM MobiCom*, 2019.
- [14] F. Adelantado, X. Vilajosana, P. Tuset-Peiro, B. Martinez, J. Melia-Segui, and T. Watteyne, "Understanding the limits of lorawan," *IEEE Communications magazine*, vol. 55, no. 9, pp. 34–40, 2017.
- [15] X. Zheng, Z. Cao, J. Wang, Y. He, and Y. Liu, "Zisense: towards interference resilient duty cycling in wireless sensor networks," in *Proceedings of SenSys*, 2014.
- [16] J. Polastre, J. Hill, and D. Culler, "Versatile low power media access for wireless sensor networks," in *Proceedings of SenSys*, 2004.
- [17] K. Jim and R. Keith, *Computer networking: A top-down approach, 7th Edition*. Pearson, 2016.
- [18] C. Li and Z. Cao, "Lora networking techniques for large-scale and long-term iot: A down-to-top survey," *ACM Computing Surveys*, 2022.
- [19] C. Li, H. Guo, S. Tong, X. Zeng, Z. Cao, M. Zhang, Q. Yan, L. Xiao, J. Wang, and Y. Liu, "Nelora: Towards ultra-low snr lora communication with neural-enhanced demodulation," in *Proceedings of ACM SenSys*, 2021.
- [20] A. Dongare, R. Narayanan, A. Gadre, A. Luong, A. Balanuta, S. Kumar, B. Iannucci, and A. Rowe, "Charm: exploiting geographical diversity through coherent combining in low-power wide-area networks," in *Proceedings of ACM/IEEE IPSN*, 2018.
- [21] Y. Peng, L. Shangguan, Y. Hu, Y. Qian, X. Lin, X. Chen, D. Fang, and K. Jamieson, "Plora: a passive long-range data network from ambient lora transmissions," in *Proceedings of ACM SIGCOMM*, 2018.
- [22] L. Liu, Y. Yao, Z. Cao, and M. Zhang, "Deeplora: Learning accurate path loss model for long distance links in lpwan," in *Proceedings of IEEE INFOCOM*, 2021.
- [23] Y. Wang, X. Zheng, L. Liu, and H. Ma, "Polartracker: Attitude-aware channel access for floating low power wide area networks," in *Proceedings of IEEE INFOCOM*, 2021.
- [24] S. Demetri, M. Zúñiga, G. Pietro Picco, F. Kuipers, L. Bruzzone, and T. Telkamp, "Automated estimation of link quality for lora: a remote sensing approach," in *Proceedings of ACM/IEEE IPSN*, 2019.
- [25] M. Hessar, A. Najafi, and S. Gollakota, "Netscatter: Enabling large-scale backscatter networks," in *Proceedings of USENIX NSDI*, 2019.
- [26] T. Elshabrawy and J. Robert, "Interleaved chirp spreading lora-based modulation," *IEEE Internet of Things Journal*, vol. 6, no. 2, pp. 3855–3863, 2019.
- [27] P. Edward, S. Elzeiny, M. Ashour, and T. Elshabrawy, "On the coexistence of lora- and interleaved chirp spreading lora-based modulations," in *Proceedings of IEEE WiMob*, 2019.
- [28] J. Chan, A. Wang, A. Krishnamurthy, and S. Gollakota, "DeepSense: Enabling Carrier Sense in Low-Power Wide Area Networks Using Deep Learning," *arXiv:1904.10607 [cs]*, 2019.
- [29] R. Piyare, A. L. Murphy, M. Magno, and L. Benini, "On-demand lora: Asynchronous tdma for energy efficient and low latency communication in iot," *Sensors*, vol. 18, no. 11, p. 3718, 2018.
- [30] C. Lesnik and A. Kawalec, "Modification of a weighting function for nlfm radar signal designing," *Acta Physica Polonica A*, vol. 114, no. 6-A, 2008.
- [31] A. W. Doerry, "Generating nonlinear fm chirp waveforms for radar." Sandia National Laboratories, Tech. Rep., 2006.
- [32] S. R. Benson, "Modern digital chirp receiver: Theory, design and system integration," 2015.
- [33] M. A. Khan, R. K. Rao, and X. Wang, "Performance of quadratic and exponential multiuser chirp spread spectrum communication systems," in *Proceedings of IEEE SPECTS*, 2013.
- [34] N. Hosseini and D. W. Matolak, "Nonlinear quasi-synchronous multi user chirp spread spectrum signaling," *IEEE Transactions on Communications*, 2021.
- [35] Q. Wang, "Non-linear chirp spread spectrum communication systems of binary orthogonal keying mode," Ph.D. dissertation, The University of Western Ontario, 2015.
- [36] A. A. Syed, W. Ye, J. Heidemann, and B. Krishnamachari, "Understanding spatio-temporal uncertainty in medium access with aloha protocols," in *Proceedings of the second workshop on Underwater networks*, 2007, pp. 41–48.
- [37] M. A. Khan, H. Ma, S. M. Aamir, and Y. Jin, "Optimizing the performance of pure aloha for lora-based esl," *Sensors*, vol. 21, no. 15, p. 5060, 2021.
- [38] D. Croce, M. Gucciardo, I. Tinnirello, D. Garlis, and S. Mangione, "Impact of spreading factor imperfect orthogonality in lora communications," in *Proceedings of Springer International Tyrrhenian Workshop on Digital Communication*, 2017.
- [39] T. Shuai, X. Zhenqiang, and W. Jiliang, "Colora: Enable muti-packet reception in lora," in *Proceedings of IEEE INFOCOM*, 2020.
- [40] S. Tong, J. Wang, and Y. Liu, "Combating packet collisions using non-stationary signal scaling in LPWANs," in *Proceedings of ACM MobiSys*, 2020.
- [41] J. S. Hunter, "The exponentially weighted moving average," *Journal of quality technology*, vol. 18, no. 4, pp. 203–210, 1986.
- [42] G. R. project, "Gnu radio website," <http://www.gnuradio.org>, Accessed 07-Apr-2020.
- [43] V. Antenna, "Vert900 vertical antenna (824-960 mhz, 1710-1990 mhz) dualband," in <https://www.ettus.com/all-products/vert900/>, Retrieved by May 10th 2021.
- [44] J. Manweiler, N. Santhapuri, S. Sen, R. R. Choudhury, S. Nelakuditi, and K. Munagala, "Order matters: Transmission reordering in wireless networks," *IEEE/ACM Transactions on Networking*, vol. 20, no. 2, pp. 353–366, 2011.
- [45] D. Tse and P. Viswanath, *Fundamentals of wireless communication*. Cambridge university press, 2005.